

## Angular-Momentum-Dependent Orbital-Free Density Functional Theory

Youqi Ke,<sup>1</sup> Florian Libisch,<sup>1</sup> Junchao Xia,<sup>1</sup> Lin-Wang Wang,<sup>2</sup> and Emily A. Carter<sup>1,\*</sup>

<sup>1</sup>*Department of Mechanical and Aerospace Engineering, Program in Applied and Computational Mathematics, and Andlinger Center for Energy and the Environment, Princeton University, Princeton, New Jersey 08544, USA*

<sup>2</sup>*Material Science Division, Lawrence Berkeley National Laboratory, Berkeley, California 94720, USA*

(Received 18 March 2013; published 9 August 2013)

Orbital-free (OF) density functional theory (DFT) directly solves for the electron density rather than the wave function of many electron systems, greatly simplifying and enabling large scale first principles simulations. However, the required approximate noninteracting kinetic energy functionals and local electron-ion pseudopotentials severely restrict the general applicability of conventional OFDFT. Here, we present a new generation of OFDFT called angular-momentum-dependent (AMD)-OFDFT to harness the accuracy of Kohn-Sham DFT and the simplicity of OFDFT. The angular momenta of electrons are explicitly introduced within atom-centered spheres so that the important ionic core region can be accurately described. In addition to conventional OF total energy functionals, we introduce a crucial nonlocal energy term with a set of AMD energies to correct errors due to the kinetic energy density functional and the local pseudopotential. We find that our AMD-OFDFT formalism offers substantial improvements over conventional OFDFT, as we show for various properties of the transition metal titanium.

DOI: [10.1103/PhysRevLett.111.066402](https://doi.org/10.1103/PhysRevLett.111.066402)

PACS numbers: 71.15.Mb, 71.20.Be

In recent years, orbital-free (OF) density functional theory (DFT) [1,2] has attracted increasing interest due to its huge advantage in numerical simplicity and efficiency: it scales linearly with system size and thus allows large scale first principles simulations not feasible today using orbital-based approaches such as Kohn-Sham (KS) DFT [3]. For example, researchers have reported OFDFT benchmark calculations of over one million atoms [4], simulated the plastic deformation of Al nanowires [5], liquid Li and Na surface structures [6], metal grain boundaries [7], multiscale simulations of nanoindentation [8], etc. However, the lack of orbitals requires the use of approximate noninteracting kinetic energy density functionals (KEDFs) and local pseudopotentials (LPSs) for representing ionic cores, often resulting in large errors compared to KSDFT. Despite great efforts in past decades to advance OFDFT via modern KEDFs [9,10] and bulk-derived local pseudopotentials (BLPS) [11], conventional OFDFT still suffers from large quantitative (or even qualitative) errors for a wide range of important materials, e.g., those containing transition metals. A substantial improvement in the accuracy and general applicability of OFDFT is therefore required to establish OFDFT as a widely adopted theory for large scale material science simulations.

Conventional OFDFT faces three major problems, which are especially severe for describing systems with localized electrons, such as transition metals. (i) Using the total electron density as the sole working variable provides no way to distinguish electrons with different angular momenta. Consequently, critically important nonlocal contributions to the exact kinetic energy (KE) and the ion-electron interaction are neglected, especially in the core region. By contrast, KSDFT includes the angular-momentum-dependent (AMD) centrifugal potential in the KE operator

and nonlocal AMD pseudopotentials (NLPS) [12] for high accuracy and transferability. (ii) Current KEDFs [9,10] contain highly nonlinear terms: the Thomas-Fermi KEDF [13]  $T_s^{\text{TF}} \propto \int \rho^{5/3} d\vec{r}$  and the von Weizsäcker KEDF [14]  $T_s^{\text{vW}} \propto \int |\nabla \rho|^2 / \rho d\vec{r}$ . While the exact KE depends linearly on the occupation of each angular momentum channel, the use of nonlinear KEDFs induces unphysical interactions between electrons of different angular momenta, resulting in errors in evaluating the KE and its potential. (iii) Modern KEDFs [9,10] reproduce the Lindhard response function in the limit of a uniform electron gas subject to small perturbations and thus are accurate mostly for nearly free-electron-like systems (e.g., simple main group metals). When applied to localized electrons (such as  $d$  electrons in transition metals), conventional OFDFT produces large errors or even qualitatively wrong behavior in the electron density and the linear response function (related to  $\delta^2 T_s^{\text{KEDF}}[\rho] / (\delta \rho)^2$  [2]), yielding wrong properties. Removing these deficiencies requires knowledge about electron angular momenta, representing a long-standing challenge for developing a general and accurate OFDFT. In this Letter, we report a general AMD-OFDFT formalism, a new generation of OFDFT, to resolve its most difficult issues. The new formalism finally allows OFDFT to accurately describe a variety of properties of transition metals featuring partially filled and highly localized  $d$ -shells.

The above deficiencies (i)–(iii) of conventional OFDFT are most dire close to the ionic cores: the nonlocal parts of pseudopotentials [12] are nonzero only within a small region around each core, and rapid electron density variations around the cores are problematic for modern KEDFs [9,10] developed for a slowly varying density found between the cores. We therefore use a muffin tin (MT)

geometry in AMD-OFDFT to divide space into two regions: an interstitial region where conventional OFDFT is applied, and atom-centered spheres where the angular momenta of electrons are explicitly taken into account. We then introduce a nonlocal energy term to effectively correct errors due to the approximate KEDF and LPS to correctly model the AMD physics in the important core region.

Using the MT geometry, we apply different strategies in different regions (see Fig. 1 and the Supplemental Material [15]): inside the MT spheres, the electron density is expanded in KS-derived atom-centered basis functions  $\psi_R$  combined with an on-site density matrix  $N_R$ , and outside by an interstitial density  $\rho_I$ , i.e.,  $\rho = \rho_I + \sum_R N_R \psi_R^* \psi_R$ . In this way, we can account for the important AMD effects of the KE operator and NLPS on the shape of  $\rho$  through  $\psi_R$ , providing an important basis to accurately describe the core region that cannot be achieved by conventional OFDFT. The OF total energy functional now becomes  $E^{\text{OF}}[\rho(\vec{r})] = E^{\text{OF}}[\{N_R\}, \rho_I(\vec{r})]$ . The use of  $N_R$  provides the angular momentum dependence inside the spheres where the AMD physics is most important. This hybrid scheme allows for explicitly including AMD energy terms that are not feasible in conventional OFDFT.

We consider a general  $E^{\text{OF}}$  as

$$E^{\text{OF}}[\{N_R\}, \rho_I] = T_s^{\text{KEDF}}[\rho] + E_{\text{XC}}[\rho] + E_H[\rho] + E_{i-e}^{\text{local}}[\rho] + E^{\text{NL}}[\{N_R\}, \rho_I], \quad (1)$$

where  $T_s^{\text{KEDF}}$ ,  $E_{\text{XC}}$ ,  $E_H$ , and  $E_{i-e}^{\text{local}}$  are the noninteracting KE, exchange-correlation, Hartree, and LPS energies, respectively. The nonlocal energy  $E^{\text{NL}}$  corrects the errors due to  $T_s^{\text{KEDF}}$  and includes AMD physics beyond  $E_{i-e}^{\text{local}}$ . A physically sensible formulation of  $E^{\text{NL}}$  is key for correct electron occupations and improved properties. Ideally,  $E^{\text{NL}}$  should contain all the differences between KS and the conventional OFDFT total energy

$$E^{\text{NL}} = E_{i-e}^{\text{NLPS}} + T_s - T_s^{\text{KEDF}}, \quad (2)$$

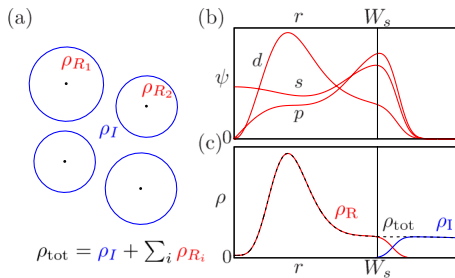


FIG. 1 (color online). (a) The muffin tin geometry partitions space into spheres centered at nuclei (sphere radius  $W_s$ ) and an interstitial region. (b) Basis functions are truncated outside the MT spheres. (c) The total density is the sum of the interstitial density  $\rho_I$  and the MT density  $\rho_R$ .  $\rho_R = \sum_{lm,l'm'} N_{R,lm,l'm'} \psi_{R,lm} \psi_{R,l'm'}^*$ , where  $l$  and  $m$  are the angular momentum and magnetic quantum numbers.

where  $E_{i-e}^{\text{NLPS}}$  is the nonlocal part of the pseudopotential energy and  $T_s$  is the exact noninteracting electron kinetic energy. We choose the MT sphere radius large enough (beyond the cutoff radii of NLPSs) so that the only  $E^{\text{NL}}$  correction remaining in the interstitial region is  $[T_s - T_s^{\text{KEDF}}]$ . We find that completely neglecting  $T_s - T_s^{\text{KEDF}}$  results in unphysical occupations inside the spheres because of errors in the KEDFs. Thus,  $T_s - T_s^{\text{KEDF}}$  must be properly treated. As demonstrated by their success in simple metals, modern KEDFs [9,10] accurately describe slowly varying electron densities. As densities should be mostly slowly varying in interstitial regions, we can safely neglect  $T_s - T_s^{\text{KEDF}}$  in the interstitial region. To ensure continuity of the KE density, we use a function to scale down the energy density of  $T_s - T_s^{\text{KEDF}}$  to zero at the sphere boundary, resulting in a rigorous hybrid KE model in which a part of the KEDF is replaced with  $T_s$  within the MT spheres (see Eq. (5) in the Supplemental Material [15]). We can then derive a general form of  $E^{\text{NL}}$  for the MT region.

As mentioned earlier, both  $T_s$  and  $E_{i-e}^{\text{NLPS}}$  in Eq. (2) depend linearly on the AM channel occupations while available model KEDFs do not. To correctly remove deficiencies of model KEDFs, i.e., unphysical implicit interactions between AM channels and errors due to use of the Lindhard response function (since the exact response function is unknown in general form), we subtract the linear and major nonlinear contributions of the model KEDF within the MT spheres as we evaluate Eq. (2). A rigorous derivation based on a Taylor expansion then yields (see the Supplemental Material [15])

$$E^{\text{NL}}[\{N_R\}] = \sum_{R,l} E_R^l N_{R,l}^{\text{total}} - \sum_{R,l} V_R^l (N_{R,l}^{\text{total}})^{5/3} - \sum_{R,l,mm'} U_R^l A_{l,mm'} \Delta N_R^{lm} \Delta N_R^{lm'} - \sum_{R,l,mm'm''} K_R^l \Lambda_{l,mm'm''} \Delta N_R^{lm} \Delta N_R^{lm'} \Delta N_R^{lm''}, \quad (3)$$

where the total occupation  $N_{R,l}^{\text{total}} = \sum_{m=-l,l} N_{R,lm,lm}$ ,  $\Delta N_R^{lm} = N_{R,lm,lm} - N_{R,l}^0$ , the average occupation  $N_{R,l}^0 = N_{R,l}^{\text{total}} / (2l + 1)$ , and  $A$  and  $\Lambda$  are constants determined by integrals over the spherical harmonics (see the Supplemental Material [15]). Note that Eq. (3) only considers diagonal elements of  $N_R$  because of the small hybridization of  $l$  channels in the core region. Although Eq. (3) is derived in the Supplemental Material [15] based on transition metals, in which the  $d$  channel dominates the ionic core region, it can easily be generalized to systems with  $s$  or  $p$  channels dominating the core region by replacing the  $d$  with  $s$  or  $p$  in the derivation.

$E_R^l$ ,  $V_R^l$ ,  $U_R^l$ , and  $K_R^l$  are on-site AMD energies obtained with the help of the basis functions (Fig. 1) by integrating over the MT spheres. Thus, the problem is reduced to finding a small set of optimal AMD energies that improve

system properties.  $V_R^l$ ,  $U_R^l$ , and  $K_R^l$  are only considered for  $l$  channels featuring localized electrons, such as the  $d$  channel in transition metals, because of their dominant contribution inside the core region. The first (linear) term of Eq. (3) includes  $E_{i-e}^{\text{NLPS}}$ ,  $T_s$ , and the linear component of  $-T_s^{\text{KEDF}}$  [15] inside the MT spheres. The form of  $N^{5/3}$  for the  $V_R^l$  term represents the leading nonlinear term in  $-T_s^{\text{KEDF}}$ , i.e.,  $T_s^{\text{TF}} \propto \int \rho^{5/3} d\tilde{r}$  [10,15].  $E_R^l$  and  $V_R^l$  are very important for the absolute value of the total energy. They also correct the relative energies between  $l$  channels inside the MT spheres as well as between electrons inside the spheres and in the interstitial region, and are thus crucial to give the correct total occupations in each  $l$  channel inside the MT spheres. The third and fourth terms containing  $U_R^l$  and  $K_R^l$  correct the delocalization error arising from intra-channel interaction errors in model KEDFs due to use of the total density as the sole variable [15,16]. These terms, especially the third term containing  $U_R^l$ , thus correctly distribute the electrons within each subchannel  $m = -l, \dots, l$ . The form of the third term looks similar to the KSDFT +  $U$  formalism [17] but accounts for different physics for the localized electrons (i.e., an improved description of the kinetic energy rather than the exchange energy). Despite their obvious physical importance, explicit derivation of  $E_R^l$ ,  $V_R^l$ ,  $U_R^l$ , and  $K_R^l$  is challenging. For now, we instead determine them by comparing to a small number of target KSDFT results. We emphasize here that only a physically sensible formulation of  $E^{\text{NL}}$  would allow such a procedure to also yield reasonable physical properties beyond the initial benchmark values. We therefore test a set of AMD energies for transferability against a group of additional properties, including defect structures such as vacancies and surfaces.

The AMD energies depend only weakly on the small occupations of the delocalized channels (such as the  $s$  and  $p$  channels in transition metals), which are sensitive to system changes (see Eqs. (17)–(20), (23), and (25) of the Supplemental Material [15]). While they do depend on the occupation of the localized channel (such as the  $d$  channel in transition metals), this occupation is rarely influenced by system changes. Therefore, the AMD energies will, to a good approximation, be constant for a given element, providing a strong basis for good transferability, as confirmed by our results below. Future work considering the explicit dependence of the AMD energies on the occupations will further enhance their transferability. The generality of our AMD-OFDFT method is not only determined by the AMD energies but also by the transferability of the KEDF model and of the fixed basis functions  $\psi_R$ . Modern KEDFs [9,10] as applied to simple metals should be accurate enough to at least describe the interstitial region in different structures of any metal, and perhaps for other materials as well. We derive  $\psi_R$  from KSDFT NLPS calculations of a suitable target system to explicitly consider the effect of the surrounding electronic structure [16].

The  $\psi_R$  obtained in this way exhibit good transferability thus far, as shown below. After obtaining the AMD energies in  $E^{\text{NL}}$  for each MT sphere, we variationally minimize  $E^{\text{OF}}[\{N_R\}, \rho_I]$  to obtain the ground state  $[\{N_R\}, \rho_I]$ . We use Lagrange multipliers to constrain the total electron number [16] and ensure the Pauli exclusion principle is satisfied for  $[\{N_R\}, \rho_I]$  by McWeeny purification [16,18]. The force on each ion can be derived as the standard Hellmann-Feynman force plus a Pulay force correction [16], which arises from the atom-centered basis functions.

As a proof of principle, here we apply the outlined AMD-OFDFT formalism to titanium, a representative transition metal of great importance in industrial applications [19]. Our benchmark KSDFT calculations are carried out in the ABINIT software package [20]. We use the WGC99 KEDF [10] in all OFDFT calculations. For further technical details, please refer to the Supplemental Material [15]. As a first step, we use an adaptive grid search method [16] to determine the AMD energies  $E_R^{l=s,p,d}$  and  $V_R^d$  [21] by considering a small set of properties. We fit to the KS occupation numbers  $N_l^{\text{fcc}}$  for each channel, the fcc equilibrium volume  $V_0^{\text{fcc}}$  and bulk modulus  $B_0^{\text{fcc}}$ , the phase ordering energy  $\Delta E_{\text{fcc-hcp}}$  between fcc and hcp, and the absolute value of the fcc total energy (underlined values in Table I). Using only  $E_R^l$  and  $V_R^d$  in the nonlocal energy term, we can reproduce most KS-NLPS benchmark properties (underlined in AMD-OF1 row in Table I), providing an important validation for the AMD-OFDFT formalism. To quantitatively reproduce also the very sensitive phase ordering energy between fcc and hcp (see the row labeled AMD-OF2 in Table I) requires corrections to the delocalization

TABLE I. Titanium equilibrium volumes ( $V_0$ ) in bohr<sup>3</sup>, bulk moduli ( $B_0$ ) in GPa, and equilibrium energies ( $E_0$ ) in eV for hcp, fcc, bcc, and sc bulk phases at different levels of theory. AMD-OF1 uses only the first two terms in Eq. (3), while AMD-OF2 applies the entire Eq. (3). The underlined properties are used in the fitting procedure.

		hcp	fcc	bcc	sc
KS-NLPS	$V_0$	116.8	116.7	116.8	126.4
	$B_0$	133	131	129	88
	$E_0$	-268.410	+0.056	+0.121	+1.042
KS-BLPS	$V_0$	113.6	113.1	114.2	134.8
	$B_0$	118	115	101	83
	$E_0$	-281.529	+0.004	+0.020	+0.752
OF-BLPS	$V_0$	96.5	97.1	97.2	111.6
	$B_0$	302	316	286	195
	$E_0$	-279.672	+0.133	+0.088	+0.810
AMD-OF1	$V_0$	115.7	<u>115.7</u>	114.4	141.2
	$B_0$	120.8	<u>128.7</u>	131.9	67.6
	$E_0$	-268.364	<u>-0.012</u>	+0.035	+0.975
AMD-OF2	$V_0$	115.2	<u>115.2</u>	114.4	131.7
	$B_0$	121.1	<u>126.8</u>	132.4	86.6
	$E_0$	-268.451	<u>+0.047</u>	+0.114	+0.693

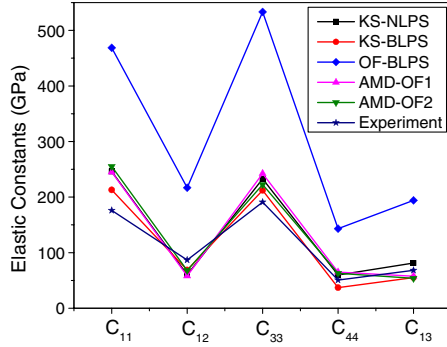


FIG. 2 (color online). The elastic constants of hcp titanium with different theories and experimental measurements [24].

errors in the KEDF, through the higher-order terms proportional to  $U_R^d$  and  $K_R^d$ . The large values of  $U_R^d$  and  $K_R^d$  underline their physical importance [21]. Note that  $U_R^d$  and  $K_R^d$  do not change the total occupations  $N_d$  but only redistribute the contribution within the different  $m$  components of  $d$ , since they account for the intrachannel interactions in the  $d$  channel.

To provide a first stringent test of the AMD-OFDFT formalism, we check the transferability of the chosen AMD energies with other properties not included in the fitting procedure: bulk properties of titanium hcp, bcc, and sc phases, as well as their phase ordering (Table I), and the  $c/a$  ratio in hcp [22]. AMD-OF2, which fully evaluates Eq. (3), produces very good agreement with KS-NLPS benchmarks for all properties investigated. To assess the accuracy gained by including AMD contributions, we also compare our results to KS-BLPS and conventional OF-BLPS theories, which use the same BLPS: the former (using the exact KE operator) accurately includes AMD effects in the kinetic energy, only neglecting the AMD contributions of the ionic cores, while conventional OF-BLPS lacks AMD contributions entirely. KS-BLPS can produce fair  $V_0$  and  $B_0$  values for all structures and qualitatively correct energy orderings between different phases. However, phase ordering energies given by KS-BLPS are too small compared to KS-NLPS benchmarks. The conventional OF-BLPS calculations produce very large errors for all properties and phases calculated: errors in  $V_0$  and  $B_0$  are as large as  $-20\%/ +200\%$  compared to KS-NLPS. In addition, OF-BLPS predicts a qualitatively wrong ordering between fcc and bcc phases. By comparing to KS-BLPS results, we can attribute the large errors in OF-BLPS to the approximate KEDF. Without properly taking into account the important AMD component of the kinetic energy, the KEDF poorly describes the electron density and response to structural changes in transition metals containing localized  $d$  electrons. The inclusion of angular momentum dependence significantly improves the accuracy of OFDFT, to the point where AMD-OFDFT is more accurate than the much more expensive KS-BLPS calculations. The nonlocal energy  $E^{\text{NL}}$  provides an effective way to correct

TABLE II. Ti hcp(0001), fcc(100), and bcc(100) surface energies: respectively,  $E_{\text{sf}}^{\text{hcp}}$ ,  $E_{\text{sf}}^{\text{fcc}}$ , and  $E_{\text{sf}}^{\text{bcc}}$  (mJ/m<sup>2</sup>) and bulk hcp Ti monovacancy formation energy  $E_{\text{vf}}$  (eV) for different levels of theory. Atomic positions are not relaxed [23].

	KS-NLPS	KS-BLPS	OF-BLPS	AMD-OF1	AMD-OF2
$E_{\text{sf}}^{\text{hcp}}$	2483	1795	5184	2145	2063
$E_{\text{sf}}^{\text{fcc}}$	2095	1655	5581	2539	2026
$E_{\text{sf}}^{\text{bcc}}$	1949	1734	6686	2692	1996
$E_{\text{vf}}$	2.73	2.12	4.49	3.04	3.06

for the kinetic energy errors. Thus, we have demonstrated that, in addition to the inclusion of NLPS effects, AMD-OFDFT can also successfully correct errors due to the approximate KEDF inside the MT spheres.

Accurately reproducing elastic moduli is an essential foundation toward simulating mechanical properties of materials. Thus, as another transferability test of the AMD energies, we calculate the elastic constants for the titanium hcp ground state structure (Fig. 2). It is clear that AMD-OFDFT greatly improves the agreement with the KS-NLPS results compared to conventional OF-BLPS theory. AMD-OFDFT produces deviations of about 10% for most  $C_{ij}$  compared to KS-NLPS.

To further assess the transferability of the AMD energies that were determined using only properties of the bulk fcc phase of Ti (underlined values in Table I), we next consider predicting properties of defect structures with precisely the same AMD-OFDFT model as before. We evaluate Ti hcp (0001), fcc(100), and bcc(100) surface formation energies  $E_{\text{sf}}$  and the monovacancy formation energy  $E_{\text{vf}}$  for the Ti hcp structure (see Table II). AMD-OFDFT predictions agree more closely with KS-NLPS theory than even KS-BLPS theory, while conventional OF-BLPS theory produces very large errors. All the above tests, including properties of bulk phases with coordination numbers changing from 12 to 6, five different types of deformations for obtaining elastic constants, and surface and vacancy formation energies, confirm the transferability of the AMD-OFDFT method.

In conclusion, we have presented and validated a novel AMD-OFDFT formalism that treats electrons of different angular momenta differently near ion cores, thereby endowing OFDFT with much greater flexibility and accuracy. The AMD effects of the KE operator and of the ion-electron interaction normally left out of OFDFT are treated here by using KSDFT-derived basis functions inside MT spheres and by introducing a crucial nonlocal energy term to effectively correct the errors in model KEDFs and LPSs. Our results for various properties of Ti show that including angular momentum dependence is essential for correct electronic structure and properties: its inclusion dramatically improves the accuracy of OFDFT. For a variety of properties we investigated, our AMD-OFDFT results agree better with KS-NLPS benchmarks than a much more

expensive KS LPS approach, even for vacancy and surface formation energies, as well as elastic constants. More sophisticated KEDFs, or a more elaborate ansatz for  $E^{\text{NL}}$ , should further improve the accuracy and transferability of AMD-OFDFT.

We gratefully acknowledge discussions with Dr. Chen Huang, Dr. Linda Hung, and Ilgyou Shin. Thanks to Dr. Mohan Chen and David B. Krisiloff for carefully reading the manuscript. This work is supported by the Office of Naval Research. We are grateful to Princeton University and DOD HPC for providing computational resources.

\*Corresponding author.

eac@princeton.edu

- [1] P. Hohenberg and W. Kohn, *Phys. Rev.* **136**, B864 (1964).
- [2] Y. A. Wang and E. A. Carter, in *Theoretical Methods in Condensed Phase Chemistry*, edited by S. D. Schwartz (Kluwer, Dordrecht, 2000), p. 117.
- [3] W. Kohn and L. J. Sham, *Phys. Rev.* **140**, A1133 (1965).
- [4] L. Hung and E. A. Carter, *Chem. Phys. Lett.* **475**, 163 (2009).
- [5] L. Hung and E. A. Carter, *J. Phys. Chem. C* **115**, 6269 (2011).
- [6] D. J. González, L. E. González, and M. J. Stott, *Phys. Rev. Lett.* **92**, 085501 (2004).
- [7] S. C. Watson and P. A. Madden, *PhysChemComm* **1**, 1 (1998).
- [8] Q. Peng, X. Zhang, C. Huang, E. A. Carter, and G. Lu, *Model. Simul. Mater. Sci. Eng.* **18**, 075003 (2010).
- [9] E. Chacón, J. E. Alvarillos, and P. Tarazona, *Phys. Rev. B* **32**, 7868 (1985); L.-W. Wang and M. P. Teter, *Phys. Rev. B* **45**, 13 196 (1992); M. Foley and P. A. Madden, *Phys. Rev. B* **53**, 10 589 (1996); P. García-González, J. E. Alvarillos, and E. Chacón, *Phys. Rev. B* **53**, 9509 (1996); **57**, 4857 (1998); V. V. Karasiev, R. S. Jones, S. B. Trickey, and F. E. Harris, *Phys. Rev. B* **80**, 245120 (2009); C. Huang and E. A. Carter, *Phys. Rev. B* **81**, 045206 (2010); **85**, 045126 (2012); J. Xia and E. A. Carter, *Phys. Rev. B* **86**, 235109 (2012).
- [10] Y. A. Wang, N. Govind, and E. A. Carter, *Phys. Rev. B* **60**, 16 350 (1999).
- [11] B. Zhou, Y. A. Wang, and E. A. Carter, *Phys. Rev. B* **69**, 125109 (2004); S. Watson, B. J. Jesson, E. A. Carter, and P. A. Madden, *Europhys. Lett.* **41**, 37 (1998); C. Huang and E. A. Carter, *Phys. Chem. Chem. Phys.* **10**, 7109 (2008).
- [12] N. Troullier and J. L. Martins, *Phys. Rev. B* **43**, 1993 (1991).
- [13] L. H. Thomas, *Proc. Cambridge Philos. Soc.* **23**, 542 (1927); E. Fermi, *Rend. Accad. Naz. Lincei* **6**, 602 (1927); *Z. Phys.* **48**, 73 (1928).
- [14] C. F. v. Weizsäcker, *Z. Phys.* **96**, 431 (1935).
- [15] See Supplemental Material at <http://link.aps.org/supplemental/10.1103/PhysRevLett.111.066402> for details of the hybrid scheme, derivation of the nonlocal energy term, and technical details for calculations.
- [16] Y. Ke *et al.* (to be published).
- [17] V. I. Anisimov, J. Zaanen, and O. K. Andersen, *Phys. Rev. B* **44**, 943 (1991).
- [18] X. P. Li, R. W. Nunes, and D. Vanderbilt, *Phys. Rev. B* **47**, 10 891 (1993).
- [19] H. M. Flower, *Nature (London)* **407**, 305 (2000).
- [20] X. Gonze *et al.*, *Comput. Phys. Commun.* **180**, 2582 (2009); *Z. Kristallogr.* **220**, 558 (2005).
- [21]  $E_R^s = -0.1133$ ,  $E_R^p = 0.02$ ,  $E_R^d = -0.38$ ,  $V_R^d = 0.1$ ,  $U_R^d = 0.252$ , and  $K_R^d = 0.5$  hartree for AMD-OF1 or 2 with a MT sphere radius = 2.2 bohr (same as  $r_{\text{cutoff}}$  for the NLPS). AMD-OFDFT gives  $N_s = 0.11$ ,  $N_p = 0.20$ , and  $N_d = 1.71$  while KS-NLPS gives  $N_s = 0.18$ ,  $N_p = 0.15$ , and  $N_d = 1.72$  within a sphere with the same radius.
- [22] The  $c/a$  ratios for the Ti hcp phase are 1.587 (KS-NLPS), 1.634 (KS-BLPS), 1.609 (OF-BLPS), 1.629 (AMD-OF1), and 1.713 (AMD-OF2). The accuracy of AMD-OF2 is acceptable compared to KS-NLPS. It is clear that  $c/a$  using AMD-OFDFT depends on the AMD energies. In the present Letter,  $c/a$  is not considered in the fitting procedure for the AMD energies but as a test of transferability.
- [23] For the monovacancy formation energy, we performed full atomic relaxation in a unit cell containing 31 Ti atoms and one empty site (since full atomic relaxation of the unit cell with 63 Ti atoms for Table II proved too time consuming using KS-NLPS). We only find 57 and 55 meV energy reductions using KS-NLPS and AMD-OF2, respectively, which are very small compared to the vacancy formation energies in Table II. The atomic relaxation for the hcp (0001) surface only reduces the surface energy by 73 mJ/m<sup>2</sup> for KS-NLPS and 35 mJ/m<sup>2</sup> for AMD-OF2. We therefore neglect the atomic relaxation for the formation energies presented in Table II.
- [24] E. S. Fisher and C. J. Renken, *Phys. Rev.* **135**, A482 (1964).